Superconductivity on a Möbius strip: Numerical studies of order parameter and quasiparticles

Masahiko Hayashi* and Hiromichi Ebisawa
Graduate School of Information Sciences, Tohoku University, Aramaki Aoba-ku, Sendai 980-8579, Japan and JST-CREST, 4-1-8, Honcho, Kawaguchi, Saitama, 332-0012, Japan

Kazuhiro Kuboki
Department of Physics, Kobe University, Kobe 657-8501, Japan
(Received 4 February 2005; published 5 July 2005)

Superconducting states of an anisotropic *s*-wave superconductor on a Möbius strip are studied numerically based on the Ginzburg-Landau theory and the Bogoliubov–de Gennes theory. In both, the equations are solved numerically on discretized lattice and the nonlinearity and the self-consistency are fully taken into account. First, we study the superconducting states on the Möbius strip in the presence of the Aharonov-Bohm flux threading the ring by employing the Ginzburg-Landau theory, and confirm the phase diagram previously proposed by Hayashi and Ebisawa [J. Phys. Soc. Jpn. **70**, 3495 (2002)]. The metastable states as well as the equilibrium state are studied and the nonequilibrium processes when the magnetic field is varied at a fixed temperature are discussed. Next, we study the microscopic superconducting states on the Möbius strip based on the Bogoliubov–de Gennes theory, especially focusing on the state with a real-space node in the superconducting gap, which is expected to appear when the flux threading the ring is close to a half-odd integer times the superconducting flux quantum. The local density of states in this *nodal state* is calculated in detail and the existence of the zero-energy bound states is shown.

DOI: 10.1103/PhysRevB.72.024505 PACS number(s): 74.20.De, 74.78.Na

I. INTRODUCTION

The realization of crystals with unusual shapes, e.g., ring, cylinder, etc., by Tanda *et al.*[1–3] has stimulated renewed interest in the effects of the system geometry on the physical properties. Especially, the synthesis of Möbius strip made of transition metal chalcogenides ($NbSe_3$, TaS_3, etc.)[4] opens a possibility to examine the physical properties of superconductivity or charge density wave in topologically nontrivial spaces.

Recently several groups have studied physical systems on Möbius strips. Hayashi and Ebisawa[5] studied *s*-wave superconducting (SC) states on a Möbius strip based on the Ginzburg-Landau (GL) theory and found that the Little-Parks oscillation, which is characteristic to the ring-shaped superconductor, is modified for the Möbius strip and a state, which does not appear for ordinary ring, shows up when the number of the magnetic flux quanta threading the ring is close to a half-odd integer. Yakubo, Avishai, and Cohen[6] have studied the spectral properties of the metallic Möbius strip with impurities and clarified statistical characteristics of the fluctuation of the persistent current as a function of the magnetic flux threading the ring. The persistent current in a more simplified version of the Möbius strip has also been studied by Mila, Stafford, and Caponi.[7] Wakabayashi and Harigaya[8] have studied the Möbius strip made of a nanographite ribbon, and the effects of Möbius geometry on the edge localized states, which is peculiar to the graphite ribbon, has been clarified. A study from a more fundamental point of view can be found in the paper by Kaneda and Okabe[9] where the Ising model on Möbius strip and its domain wall structures are studied.

The main result of Ref. 5 is that if the magnetic flux threading the ring is close to a half-odd integer times the flux quantum $\phi_0=hc/(2e)$ (h, c, e being the Planck constant, the speed of light, and the electron charge, respectively), a characteristic SC state appears. This state has a real-space node in SC gap along the circumference of the strip: namely, the gap tends to zero along the line located in the middle of the strip. Throughout this paper we call this state the "*nodal state*." It has been shown that the free energy of this state can be lower than that of uniformly gapped state, which is known to be the most stable state in case of the ordinary SC rings.

This paper extends the previous study in the following two points.

(a) In Ref. 5, we have shown that the free energy of the *nodal state* is lower than other likely states. However, there is no evidence that it is the most stable. Although it is difficult to examine all possible local-minimum states of the nonlinear GL free energy, in this paper we try to give a more convincing evidence by resorting to a numerical method. We perform numerical minimization of the GL free energy and find as many local-minimum states as possible and reexamined the phase diagram of Ref. 5. A similar method is previously employed, for example, in Refs. 10 and 11 in studying SC disks, etc.

(b) The electronic states, which are not treated in Ref. 5, are studied in terms of the Bogoliubov–de Gennes (BdG) theory. We numerically solve the BdG equation on a lattice self-consistently, where electrons are treated by the tight-binding approximation. Based on the solution we study the local density of states in the *nodal state*, which may be observed, for example, by scanning tunneling microscope measurement.

This paper is organized as follows. In Sec. II, we review the behavior of a SC Möbius strip in a magnetic field, presented in Ref. 5. In Sec. III, the model, method, and results of the numerical analyses of GL theory are presented. In Sec.

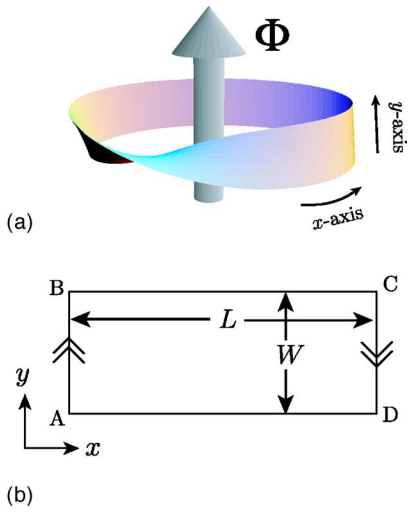

FIG. 1. (Color online) (a) Geometry of SC Möbius strip where an AB flux is threading the ring. The "x axis" and the "y axis" indicate the direction of the orthogonal coordinated set on the strip. (b) A figure obtained by cutting and spreading the Möbius strip on a flat surface. The points A and B are identified with C and D, respectively. The dashed line indicates a closed path along the x axis, which winds twice in the direction of the arrows before coming back to the initial point.

IV, studies based on the BdG theory for the electronic properties of the *nodal state* are presented. In Sec. V, discussions on the results and their relation to experiments are given. Section VI is devoted to summary.

II. A SUPERCONDUCTING MÖBIUS STRIP IN A MAGNETIC FIELD

Here we summarize the results obtained in Ref. 5. In that paper, the behavior of a SC Möbius strip in an external magnetic field is studied based on the GL theory.

We consider the Möbius strip made of a superconductor as shown in Fig. 1(a). The magnetic field is assumed to be threading the ring in a form of the so-called Aharonov-Bohm (AB) flux as indicated in the figure by a bold arrow, which gives rise to a nonzero vector potential on the strip although the magnetic field is vanishing on the strip. In actual Möbius strip, the crystal is expanded in the edges and contracted in the center. Therefore elastic deformations are inevitable. In this paper we assume that the circumference of the strip is long enough as compared to the width that the elastic deformation is negligible. Then we can set an approximately orthogonal two-dimensional coordinate on the strip as indicated in the developed figure, Fig. 1(b). We take the x and y axis along and perpendicular to the circumference, respectively. In this coordinate system, one must rotate along the x axis twice to come back to the initial point because of the twisting due to the Möbius geometry. Such a path is indicated in Fig. 1(b). We denote the circumference and the width by L and W, respectively. We further assume that the coherence length along and that perpendicular to the circumference of the strip, respectively denoted as $\xi_{\parallel}$ and $\xi_{\perp}$, are different.

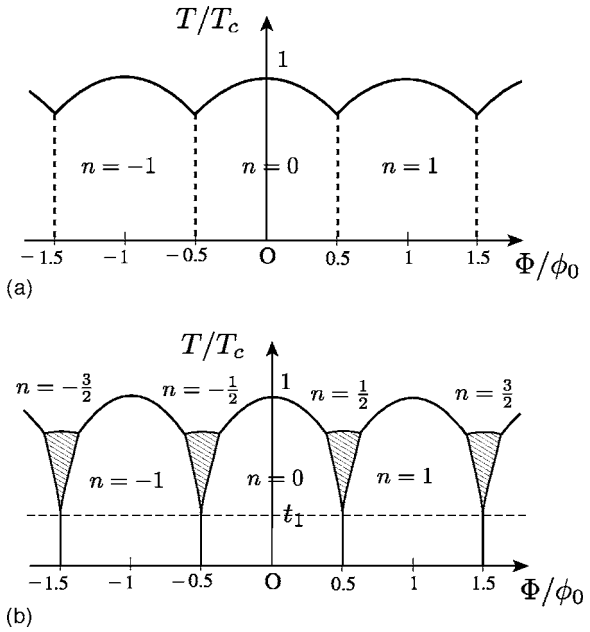

FIG. 2. Phase diagram of a superconducting Möbius strip in the presence of a AB flux with (a) $\pi r_{\parallel}/2\sqrt{3} < r_{\perp}$ and (b) $\pi r_{\parallel}/2\sqrt{3} > r_{\perp}$.

In this paper the effects of the bending, or the nonzero curvature caused in the strip by the Möbius geometry on the electronic properties are neglected. Namely, the Möbius geometry is taken into account only by the boundary condition. Although these effects may be important in case of unconventional pairing, such as p-wave superconductors,[12] they may be neglected for s-wave superconductors, which we treat in this paper.

In addition, we assume that the magnetic field is applied in the direction shown in Fig. 1(a) and the flux exists only inside the ring. The situations change if the magnetic field is applied in other directions because of the complicated three-dimensional structure of the Möbius strip. Some related problems are studied by Vodolazov and Peeters in the case of "eight figure" rings.[13]

The equilibrium states of SC Möbius strip depends on the magnetic flux Φ threading the ring. The SC Möbius strip shows the so-called Little-Parks oscillation of the transition temperature with a period ϕ_0, as we naively expect from the analogy to the ordinary rings. However, it turned out that the oscillation can be appreciably modified in SC Möbius strip depending on the strength of the anisotropy of the coherence lengths.

The analysis of Ref. 5 shows that there are two important parameters, which are given by

$$r_{\perp} = \frac{\xi_{\perp}(0)}{W}, \quad r_{\parallel} = \frac{\xi_{\parallel}(0)}{L}, \tag{1}$$

where $\xi_{\perp}(0)$ and $\xi_{\parallel}(0)$ are the coherence lengths at absolute zero temperature ($T=0$).

It has been shown that when the condition $\pi/2\sqrt{3}r_{\parallel} < r_{\perp}$ is satisfied, the phase diagram in a magnetic field behaves like the one shown in Fig. 2(a), which is basically the same

as that for the ordinary ring. Here T_c is the transition temperature in the bulk and the index n indicated in the figure denotes the winding number of the phase as we go around the ring once along a trajectory parallel to the edge. When

$$\frac{\pi}{2\sqrt{3}} r_{\parallel} > r_{\perp} \tag{2}$$

is satisfied, states characteristic to the Möbius geometry appear when the number of the flux quantum threading the ring is close to a half-odd integer, as shown in Fig. 2(b) by hatched regions. These states are indexed with a half-odd integer n and the phase of the order parameter changes by an odd number times π as we go around ring once. The spatial dependence of the order parameter is shown in Fig. 3, where the real part, the imaginary part, and the amplitude are shown for $n=1/2$ case. It is clear that the order parameter has a real-space node in the middle of the strip. Therefore we call these states the "*nodal states.*" The *nodal states* can exist above t_1 shown in Fig. 2(b). Here t_1 is given by

$$t_1 = 1 - \left(\frac{3\pi^2}{4\sqrt{2}} \frac{r_{\parallel}^2}{r_{\perp}} \right)^2 \tag{3}$$

as one can see from the results in Ref. 5.

The results of Ref. 5 are obtained by comparing the free energies of the several possible states, which are chosen empirically. Therefore it is not easy to say that there are no states with lower free energies. Of course, it is impossible to investigate all possible order parameter configurations. However, more reliable analysis, which can cover wider range of the configuration space is required. In this paper, to fulfill this requirement, we perform numerical study on GL theory, which is given in Sec. III.

The analysis of Ref. 5 is limited to the phenomenological one. Since the *nodal state* is also interesting from electronic points of view, more microscopic study is required. We solve BdG equations on the Möbius strip numerically and clarify the electronic bound state near the node of the *nodal state*. This will be given in Sec. IV.

III. NUMERICAL STUDY BASED ON GINZBURG-LANDAU THEORY

In this section, we study the SC state on the Möbius strip numerically using the GL theory. Here we employ nonlinear optimization method (quasi-Newton method) to find the local minimum state of the GL free energy.[14]

GL free energy F of our system is given as follows:

$$F = d_{\perp} \int d^2\vec{r} \left\{ \frac{\hbar^2}{2m^*} \left[\left| \left(\frac{\partial}{\partial x} - i\frac{2\pi}{\phi_0} A_x \right) \psi \right|^2 + \gamma^2 \left| \left(\frac{\partial}{\partial y} - i\frac{2\pi}{\phi_0} A_y \right) \psi \right|^2 \right] + \alpha_0 (t-1) |\psi|^2 + \frac{\beta}{2} |\psi|^4 \right\}. \tag{4}$$

The integral is over the flat two-dimensional area of Fig. 1(b) and the vector components of $\vec{A}(\vec{r})$ are defined in the same coordinate system. The constants $m^*, \phi_0 = hc/(2e)$ are the mass of a Cooper pair (twice the electron mass) and the magnetic flux quantum, respectively. The thickness of the strip $d_{\perp}$ is much smaller than the SC coherence length and the strip can be treated as two dimensional. $\psi(\vec{r})$ and $\vec{A}(\vec{r})$ are the SC order parameter and the vector potential, respectively. $t=T/T_c$ is the reduced temperature. α_0 and β are positive constants, and $\gamma = \xi_{\perp}/\xi_{\parallel}$ is the anisotropy parameter.

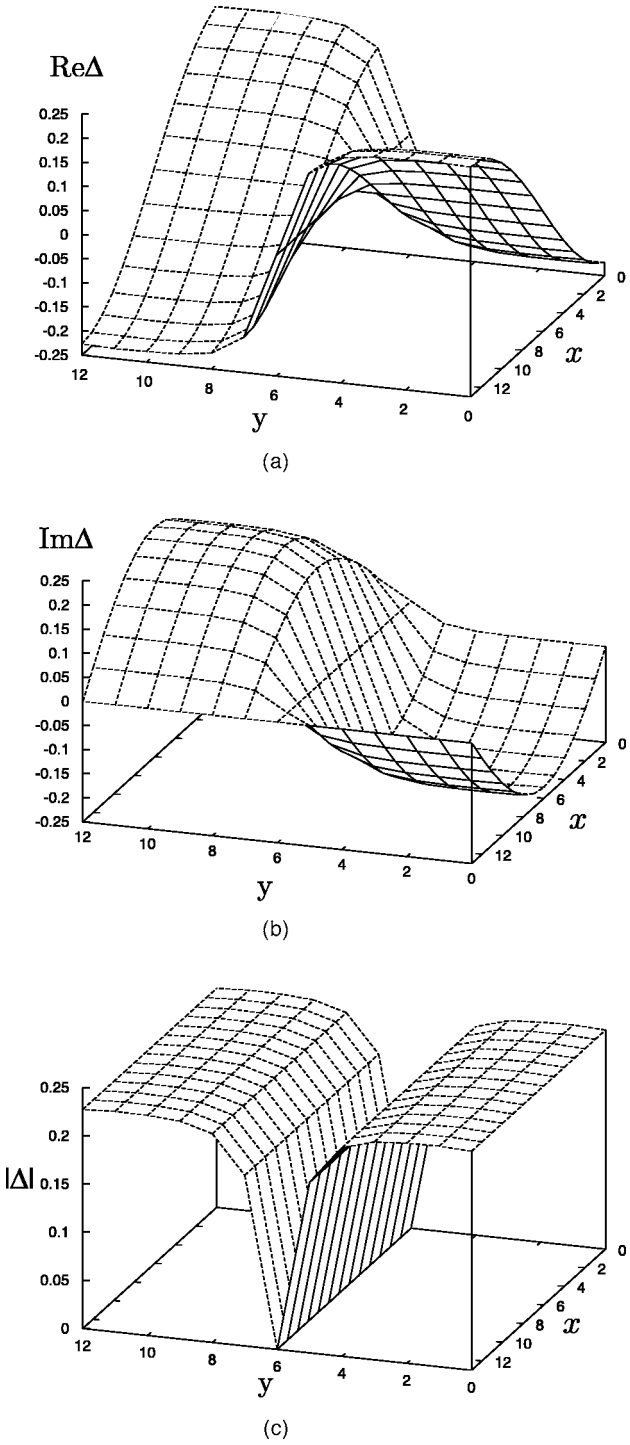

FIG. 3. (a) Real part, (b) imaginary part, and (c) amplitude of the order parameter in the *nodal state*.

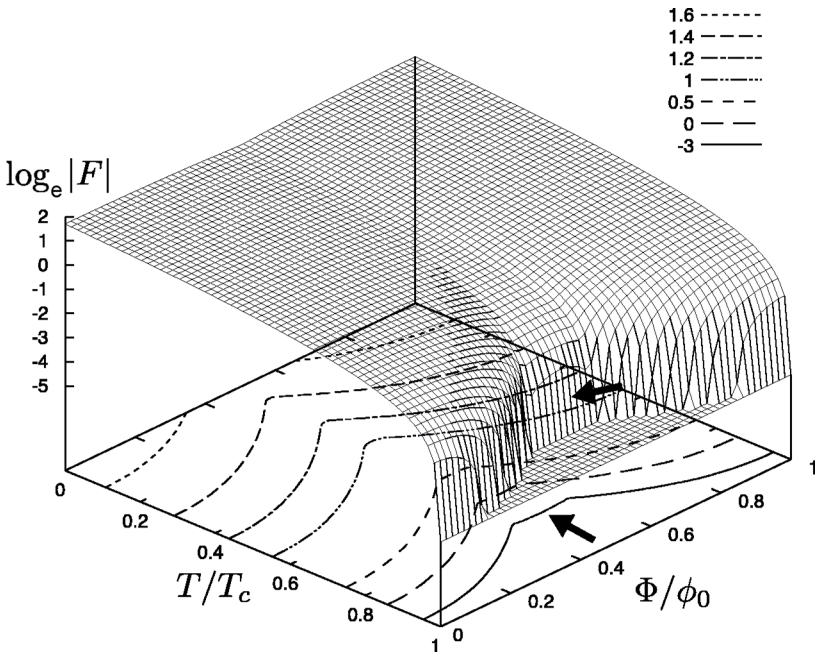

FIG. 4. (Color online) The free energy of the most stable state as a function of T and Φ. Around $\Phi \simeq \phi_0/2$ a structure corresponding to the *nodal state* can be seen. The vertical axis is the logarithm of the $|F|$ and the region with $|F| < 10^{-5}$ near T_c has been cutoff. The free energy is measured in the unit of F_0.

Here we should note the setting of the vector potential. The AB flux is incorporated by taking $\vec{A}=\Phi/L\vec{e}_x$, where $\vec{e}_x$ is the unit vector in x direction. This comes from the fact that the following relation should be satisfied:

$$\oint_{C^2} \vec{A}\cdot d\vec{r} = 2\Phi, \tag{5}$$

where C^2 means that the integral is carried out along a closed loop on a Möbius strip, such as the one shown in Fig. 1(b), which winds twice.

For numerical calculations we introduce the lattice version of F as

$$F = F_0\Bigg\{\sum_{j=1}^{N_x}\sum_{k=1}^{N_y}\tilde{\xi}^2[|\tilde{\psi}(j,k)|^2 + |\tilde{\psi}(j+1,k)|^2 - \tilde{\psi}^*(j,k)\tilde{\psi}(j+1,k)\times e^{-i\tilde{a}_x} - \text{c.c.}] + \gamma^2\sum_{j=1}^{N_x}\sum_{k=1}^{N_y-1}\tilde{\xi}^2|\tilde{\psi}(j,k)-\tilde{\psi}(j,k+1)|^2 + \sum_{i=1}^{N_x}\sum_{j=1}^{N_y}\left[(t-1)|\tilde{\psi}(j,k)|^2 + \frac{1}{2}|\tilde{\psi}(j,k)|^4\right]\Bigg\}, \tag{6}$$

where $\tilde{a}_x = 2\pi d A_x/\phi_0$, $\tilde{\xi}=\xi_{\parallel}(0)/d$, $\xi_{\parallel}(0)=\sqrt{\hbar^2/2m^*\alpha_0}$ and d is the lattice spacing. Here the lattice is assumed to be a square one. Note that $N_x d=L$ and $N_y d=W$. F_0 is $V_0\alpha^2/\beta$ where $V_0=d^2\times d_\perp$. The order parameter $\tilde{\psi}$ is normalized so that $\tilde{\psi}\to 1$ as $t\to 0$.

In order to incorporate the Möbius geometry, we put

$$\tilde{\psi}(N_x+1,k) = \tilde{\psi}(1,N_y+1-k) \tag{7}$$

$(1\leqslant k\leqslant N_y)$ in the first two lines of Eq. (6).

The order parameter $\tilde{\psi}(j,k)$ minimizing F is obtained by solving the equation

$$\frac{\partial F}{\partial \tilde{\psi}^*(j,k)} = 0, \tag{8}$$

which yields

$$\tilde{\xi}^2[-\tilde{\psi}(j+1,k)e^{-i\tilde{a}_x} - \tilde{\psi}(j-1,k)e^{i\tilde{a}_x} - \gamma^2\tilde{\psi}(j,k+1) - \gamma^2\tilde{\psi}(j,k-1) + 2(1+\gamma^2)\tilde{\psi}(j,k)] + (t-1)\tilde{\psi}(j,k) + |\tilde{\psi}(j,k)|^2\tilde{\psi}(j,k) = 0. \tag{9}$$

We obtained the solution of Eq. (9) in terms of the nonlinear optimization of the free energy Eq. (6). In this paper we especially utilized the so-called quasi-Newton method.[14] Like other methods of nonlinear optimization, quasi-Newton method starts from an initial value of $\tilde{\psi}$ and changes it so that the free energy becomes lower until finally we reach the local minimum. Therefore which local minimum we reach depends on the initial value of $\tilde{\psi}$. In this paper we randomly chose the initial values and performed optimization as many times as possible. Then we obtained several local-minimum states. These procedure is the same as the one adopted in Refs. 10 and 11.

The results are as follows. The system size we used is $N_x=10$, $N_y=10$, $\xi_0=1.5d$, and $\xi_\perp=1.2d$.

First we discuss the phase diagram. The numerically obtained free energy is shown in Fig. 4 using the log scale: we have shown only the region with $F<0$ and $\log|F|$ is plotted as a function of Φ and T. We can see from this figure that the structure corresponding to the *nodal state* appears near $\Phi=\phi_0/2$ (shown by bold arrows). Actually, the order parameter in this region behaves like that shown in Fig. 3.

In Fig. 5, we have depicted the free energies of the metastable states at three different temperatures [(a) $t=0.78$, (b) $t=0.5$, and (c) $t=0.1$]. We clearly see three distinct series of states in each graph. The branch which starts from $\phi=0$ corresponds to the state with a uniform order parameter

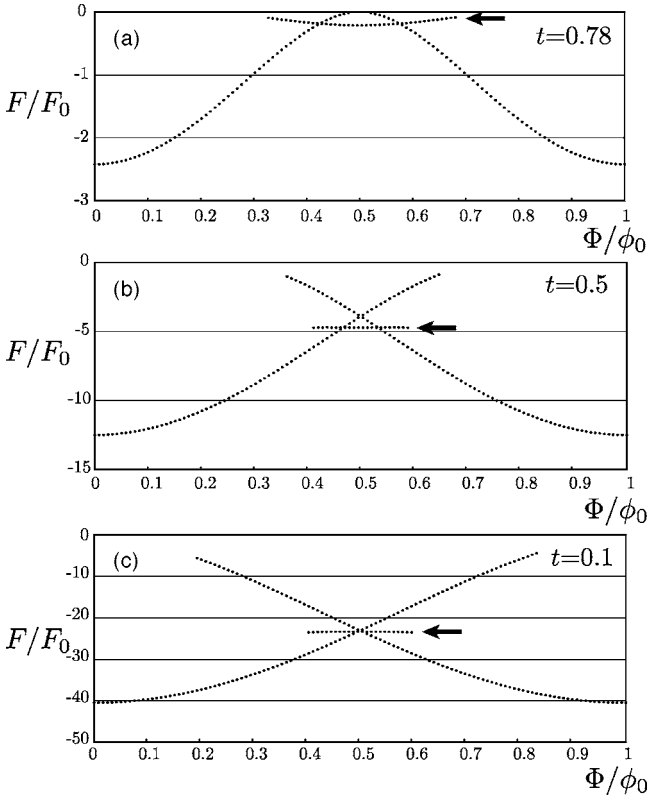

FIG. 5. The free energy of the metastable states as a function of Φ for (a) $t=0.78$, (b) $t=0.5$, and (c) $t=0.1$. The branches corresponding to the *nodal states* are indicated by bold arrows in every graph. They become the most stable state when $t=0.78$ and 0.5 for a certain region of Φ. When $t=0.1$ there is no stable region for the *nodal state*.

$\Delta=$(const.) and that ends at $\phi=\phi_0$ corresponds to the state with $\Delta=$(const.)$\times e^{i2\pi x/L}$. Between these two branches, a branch corresponding to the *nodal state* can be seen. At $t=0.78$ and $t=0.5$, the *nodal state* has the lowest free energy near $\phi\simeq\phi_0/2$. However, at $t=0.1$, although the *nodal state* is still a metastable state, there is no region where the *nodal state* is the most stable. These features agree with the prediction of Ref. 5.

IV. NUMERICAL STUDY BASED ON BOGOLIUBOV–DE GENNES THEORY

In order to study the *s*-wave SC state on a Möbius strip microscopically, we treat a tight-binding model on a square lattice with attractive on-site interactions. The Hamiltonian of the system is given by

$$H=-t_x\sum_{j\sigma}(e^{i\phi_x}c^{\dagger}_{j+\hat{x},\sigma}c_{j,\sigma}+e^{-i\phi_x}c^{\dagger}_{j,\sigma}c_{j+\hat{x},\sigma})-t_y\sum_{j\sigma}(c^{\dagger}_{j+\hat{y},\sigma}c_{j,\sigma}+c^{\dagger}_{j,\sigma}c_{j+\hat{y},\sigma})-V\sum_j n_{j\uparrow}n_{j\downarrow}-\mu\sum_{j\sigma}c^{\dagger}_{j,\sigma}c_{j,\sigma}, \tag{10}$$

where $c_{j\sigma}$ is the annihilation operator of electron at the site j with spin $\sigma(=\uparrow,\downarrow)$. $V(>0)$ and μ are the strength of the attractive interaction and the chemical potential, respectively. $j=(j_x,j_y)$ $(1\leqslant j_x\leqslant N_x, 1\leqslant j_y\leqslant N_y)$ numbers the sites, where N_x and N_y are the numbers of sites along the x and y axis, respectively, and $\hat{x}=(1,0)$, $\hat{y}=(0,1)$. $n_{j\sigma}=c^{\dagger}_{j\sigma}c_{j\sigma}$ is the electron number operator. The transfer integrals in x and y direction are denoted as t_x and t_y, respectively. The Peierls phase $\phi_x=(\pi/N_x)(\Phi/\phi_0)$ represents the effect of the AB flux Φ threading the Möbius strip. To realize the Möbius geometry we put

$$c_{(N_x+1,j_y),\sigma}=c_{(1,N_y-j_y+1),\sigma}. \tag{11}$$

The interaction term is decoupled within a mean-field approximation as

$$n_{j\uparrow}n_{j\downarrow}\rightarrow\Delta_j c^{\dagger}_{j\downarrow}c^{\dagger}_{j\uparrow}+\Delta^{*}_j c_{j\uparrow}c_{j\downarrow}-|\Delta_j|^2 \tag{12}$$

with $\Delta_j\equiv\langle c_{j\uparrow}c_{j\downarrow}\rangle$ being the SC order parameter. Then the mean-field Hamiltonian is written as

$$\mathcal{H}_{\mathrm{MFA}}=\sum_j\sum_k\Psi^{\dagger}_j h_{jk}\Psi_k, \tag{13}$$

where

$$h_{jk}=\begin{bmatrix}W_{jk} & F_{jk}\\ F^{*}_{jk} & -W_{jk}\end{bmatrix},\quad \Psi_j\equiv\begin{bmatrix}c_{j\uparrow}\\ c^{\dagger}_{j\downarrow}\end{bmatrix} \tag{14}$$

with

$$W_{jk}=-t_x(e^{i\phi_x}\delta_{k,j+\hat{x}}+e^{-i\phi_x}\delta_{k,j-\hat{x}})-t_y(\delta_{k,j+\hat{y}}+\delta_{k,j-\hat{y}})-\mu\delta_{jk},$$

$$F_{jk}=-\Delta_j\delta_{jk}. \tag{15}$$

By solving the following BdG equation:

$$\sum_l h_{jl}\begin{pmatrix}u_{ln}\\ v_{ln}\end{pmatrix}=E_n\begin{pmatrix}u_{jn}\\ v_{jn}\end{pmatrix} \tag{16}$$

we can obtain the energy eigenvalues E_n and the corresponding eigenfunctions (u_{jn},v_{jn}), where n is numbering the states. The unitary transformation using (u_{jn},v_{jn}) diagonalizes $\mathcal{H}_{\mathrm{MFA}}$, and the SC order parameter Δ_j can be written in terms of E_n and (u_{jn},v_{jn}). These constitute the self-consistency equations which will be solved numerically. In the following we take the parameters as:

$$t_x=1.0,\quad t_y=0.49,\quad \mu=0,\quad T=0.22,\quad V=0.25. \tag{17}$$

First we estimate the correlation lengths, $\xi_{\parallel}(0)$ and $\xi_{\perp}(0)$, by calculating the anomalous Green's function $F(j)\equiv\langle c_{k\downarrow}c_{k+j\uparrow}\rangle$ at $T=0$ without applying the magnetic flux, and the results are depicted in Fig. 6. (This calculation has been carried out in a larger system with 100×100 sites using periodic boundary condition for both x and y directions.) From the results in Fig. 6 and the relation $F(j)\propto\exp(-|j|/\xi)$, $\xi_{\parallel}(0)$ and $\xi_{\perp}(0)$ are estimated as

$$\xi_{\parallel}(0)=2.37d,\quad \xi_{\perp}(0)=0.64d, \tag{18}$$

where d is the lattice spacing.

The calculation in the Möbius geometry is carried out for a system with $N_x=13$ and $N_y=14$. Putting $L=13d$ and $W=14d$, we obtain $r_{\parallel}=0.18$ and $r_{\perp}=0.046$. These values satisfy the condition, Eq. (2). Furthermore, t_1 is estimated to be -13,

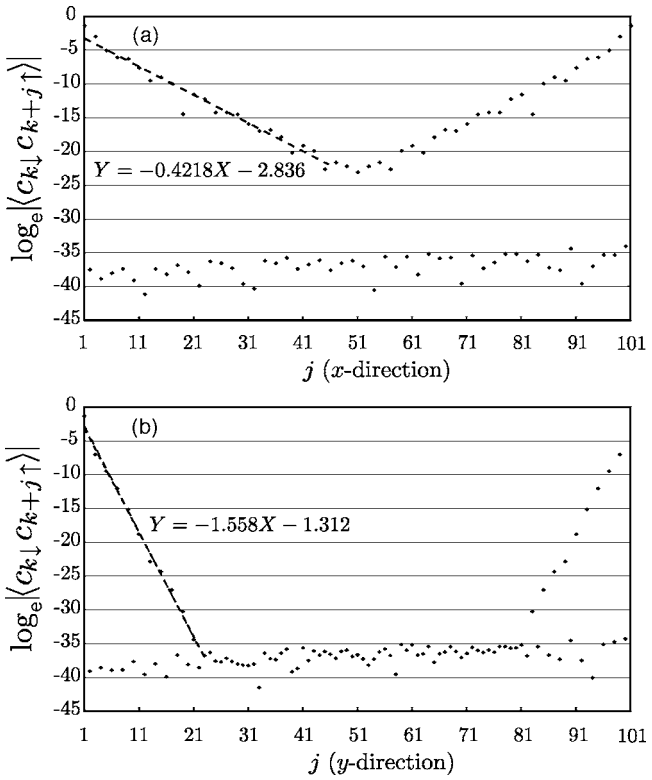

FIG. 6. The anomalous correlation function $\langle c_{k\downarrow} c_{k+j\uparrow}\rangle$ for the system with the parameters in Eq. (17). (a) and (b) correspond to the correlation in the x and y direction, respectively. The equations in the figures are the approximating lines to the exponential decay.

which means that the *nodal state* is stable at all temperature range down to 0 K. In passing, the bulk T_c of this system is 0.358 (estimated numerically in the system with 100×100 sites), which coincides with that in 13×14 system with $\Phi = 0$ within numerical accuracy.

In this calculation, we limited ourselves to the case of the *nodal state* at $\phi = \phi_0/2$. Since this microscopic calculation needs more time to obtain good convergence as compared to the GL calculation, we have selected for the initial order parameter the solution obtained by the GL analysis, such as the one depicted in Fig. 3. After the calculation, the behavior of the order parameter has not changed so much and we considered that the iteration converged to the *nodal state*. The local density of states (LDOS) is calculated from the equation

$$N(j,E) = -\frac{1}{\pi}\mathrm{Im}\sum_n \frac{u_{jn}^* u_{jn}}{E - E_n + i\Gamma}, \tag{19}$$

where Γ is the broadening of the single energy level, introduced to simulate the actual experiment. The result is shown in Fig. 7 with $\Gamma = 0.03$. Each line of Fig. 7 corresponds to the LDOS at $j = (1, j_y)$ where j_y numbers the chain from the edge of the strip. (The LDOS is independent of j_x.) Because of the inversion symmetry with respect to the center, we depicted LDOS only for $1 \leqslant j_y \leqslant 7$, where $j_y = 1$ and $j_y = 7$ correspond to the outermost and the innermost chain, respectively.

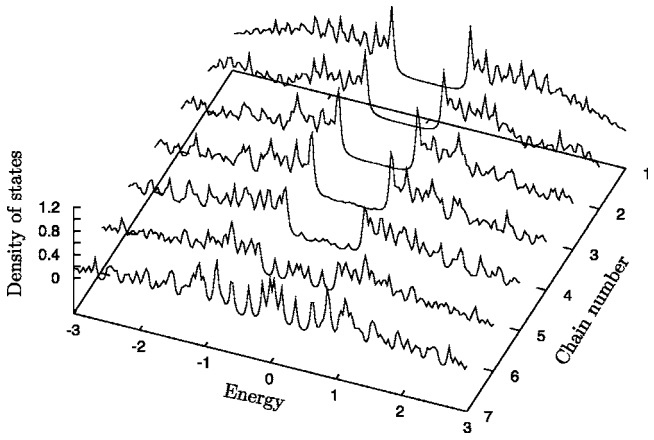

FIG. 7. The local density of state in the *nodal state* on the Möbius strip

In Fig. 7, a well-developed gap behavior can be seen for $1 \leqslant j_y \leqslant 5$ and the bound states are formed in the chains $j_y = 6$ and 7. These bound states originates from the node. Since the node can be regarded as the spontaneously formed π junction (as one can see from Fig. 3, the phase of the order parameter changes by π in crossing the node), the bound state energy is expected to be zero. However, in Fig. 7, the deviation from zero energy is seen. The phase variation along the node line, which does not exist for the ordinary Josephson junctions, may be important for this phenomenon. We have confirmed numerically that the deviation is smaller for the systems with larger circumferences and thus it is likely to be a finite-size effect. This point will be discussed in detail in a separate paper.[15]

V. DISCUSSION

In this paper, by using the numerical methods, we have confirmed that the predictions of Ref. 5 are satisfied within both GL and BdG level. Until now, we have limited our discussion to purely two-dimensional cases. This is not the case for actually synthesized Möbius crystals.[4] Here we discuss the effects of the finite thickness of the strip. If the Möbius strip is thicker than the SC coherence length, the *nodal state* may no longer be stable and the node, which is obtained under the assumption that the gap is uniform in the direction of the thickness, may become a vortex line embedded inside the strip. Then there is no gapless region on the surface. In this case, we cannot observe the node by only measuring the surface density of states by scanning tunneling microscope. Even then the observation of the *nodal state* may be possible through measurement of the variation of the gap or the magnetization as a function of the magnetic flux. More precise analysis on the thicker Möbius strips is left for the future study.

In Sec. III, we have calculated the free energies not only of the equilibrium state but also of the metastable states. The metastable states do not appear in the thermodynamic equilibrium, though they play important roles in actual experiments in which one sweeps the magnetic flux.[16–19] As shown by the previous studies, when we change the magnetic flux

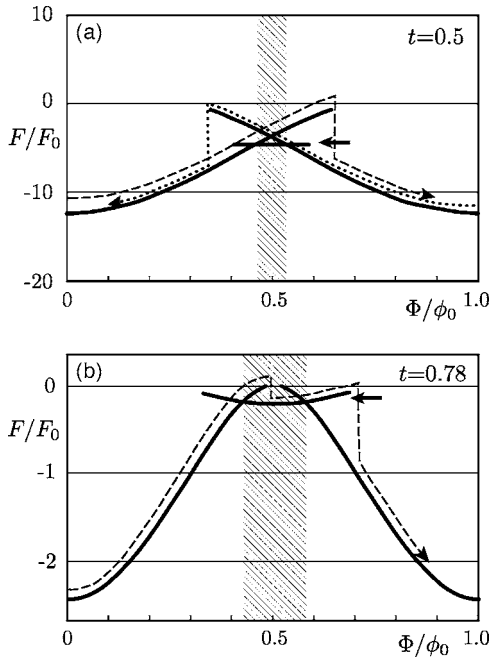

FIG. 8. The transition of the states in the field sweep experiment for (a) $t=0.5$ and (b) $t=0.78$. The *nodal state* is the most stable in the shaded region. See text for details.

the state of the system remains in one of the metastable states and it does not switch to another lower-energy state until the initial state finally becomes unstable. Although there may be an effect of thermally assisted tunneling, such effects are limited to the very vicinity of the critical temperature. From these we point out a possibility that the *nodal state* may not appear at all in the field sweep experiment even though it can be a true equilibrium state for some values of the flux. This is understood from Fig. 8(a), where the free energy for $t=0.5$ and the time evolution of the system under a field sweep process are shown. The bold curves show the free energies of the metastable states and the equilibrium state at $t=0.5$. The branch corresponding to the *nodal state* is indicated by a bold arrow. The dashed and dotted curves show the time evolution of the system in up-sweep and down-sweep experiment, respectively, where it is assumed that the transition between different branches are prohibited by the energy barrier except when the system comes to the end of a branch. In this case, although the *nodal state* can be a true equilibrium state, it does not appear during the field sweep process. In contrast to this, the *nodal state* appears during the field sweep process at $t=0.78$, as shown in Fig. 8(b) (only the up-sweep process is indicated). Because of these reasons, the observability of the *nodal state* in the field-sweep experiment may be further limited to the region in the vicinity of the critical temperature. More precise numerical simulations are required to clarify these dynamical processes quantitatively, which are left for future studies.

VI. SUMMARY

In this paper, we have investigated the superconducting states on a Möbius strip in terms of the numerical analyses based on Ginzburg-Landau and Bogoliubov–de Gennes theory. It has been shown that in the Möbius geometry a *nodal state* can appear both in equilibrium and metastable states. The experimental observability of the *nodal states* is discussed based on the findings.

ACKNOWLEDGMENTS

M.H. and H.E. were financially supported by Grants-in-Aid for Scientific Research of Ministry of Education, Science, and Culture. K.K. was financially supported by the Sumitomo Foundation.

*Electronic address: hayashi@cmt.is.tohoku.ac.jp

[1] S. Tanda, H. Kawamoto, M. Shiobara, Y. Okajima, and K. Yamaya, J. Phys. IV **9**, 379 (1999).
[2] S. Tanda, H. Kawamoto, M. Shiobara, Y. Sakai, S. Yasuzuka, Y. Okajima, and K. Yamaya, Physica B **284-288**, 1657 (2000).
[3] Y. Okajima, H. Kawamoto, M. Shiobara, K. Matsuda, S. Tanda, and K. Yamaya, Physica B **284-288**, 1659 (2000).
[4] S. Tanda, T. Tsuneta, Y. Okajima, K. Inagaki, K. Yamaya, and N. Hatakenaka, Nature (London) **417**, 397 (2002).
[5] M. Hayashi and H. Ebisawa, J. Phys. Soc. Jpn. **70**, 3495 (2002).
[6] K. Yakubo, Y. Avishai, and D. Cohen, Phys. Rev. B **67**, 125319 (2003).
[7] F. Mila, C. A. Stafford, and S. Capponi, Phys. Rev. B **57**, 1457 (1998).
[8] K. Wakabayashi and K. Harigaya, J. Phys. Soc. Jpn. **72**, 998 (2003).
[9] K. Kaneda and Y. Okabe, Phys. Rev. Lett. **86**, 2134 (2001).
[10] V. A. Schweigert, F. M. Peeters, and P. S. Deo, Phys. Rev. Lett. **81**, 2783 (1998).
[11] B. J. Baelus, F. M. Peeters, and V. A. Schweigert, Phys. Rev. B **61**, 9734 (2000).
[12] M. Sigrist and K. Ueda, Rev. Mod. Phys. **63**, 239 (1991).
[13] D. Y. Vodolazov and F. M. Peeters, Physica C **400**, 165 (2004).
[14] W. H. Press, B. P. Flannery, S. A. Teukolsky, and W. T. Vetterling, *Numerical Recipes in C* (Cambridge University Press, Cambridge, 1988).
[15] T. Suzuki, M. Hayashi, H. Ebisawa, and K. Kuboki (unpublished).
[16] B. J. Baelus, F. M. Peeters, and V. A. Schweigert, Phys. Rev. B **63**, 144517 (2001).
[17] V. A. Schweigert and F. M. Peeters, Phys. Rev. Lett. **83**, 2409 (1999).
[18] A. Kanda and Y. Ootuka, Physica B **329-333**, 1421 (2003).
[19] A. Kanda and Y. Ootuka, Physica C **404**, 205 (2004).